

**Synthesis, characterization and cytotoxic activity of**

**N-(5-indanyl(methylene)anthranilic acid(5-indanyl methylene)-hydrazide and its  
Pt(II) complex**

**Abstract** A new platinum complex of N-(5-indanyl(methylene)anthranilic acid(5-indanyl methylene)-hydrazide (HL) has been synthesized and characterized by physical and spectral techniques, as elemental analysis, IR, EI-MS, <sup>1</sup>H-NMR, thermal analysis, transmittance electron microscope (TEM) and magnetic moment. The results indicated that the ligand binds to Pt(II) in the enol form. Square-planar stereochemistry was suggested for the Pt(II) complex. The morphological characterization showed nano-sized spherical particles with average size 92 nm of the isolated complex. The synthesized Pt(II) complex exhibited a significant cytotoxic activity against HCT116 and HEPG2. Also *in vivo* study of the Pt(II) complex showed cytotoxic activity towards Ehrlich ascites carcinoma (EAC).

**Keywords** Synthesis. Pt(II) complex. Cytotoxic activity

---

**Introduction**

Cancer is the major serious problem which causes death all over the world. The cause of cancer is attributed to genetic damage to the cells. The damaged cells do not respond to normal tissue controls. The affected cells multiply rapidly to cause spread of cancer and formation of varying degrees of tumors ([Zhukova and Dobrynin, 2001](#)).

The discovery of effective new cancer therapies is a strong demand. Since the discovery of the platinum based complex, cisplatin, in 1965 ([Divsalar et al., 2013](#)), medicinal inorganic chemistry has attracted much more attention and a large number of platinum complexes with promising pharmacological properties have been synthesized ([Kostova, 2006](#)). The cytotoxic action mechanism of many metal complexes has been discussed aiming to develop new anti-tumor agents ([Grunicke et al., 2006](#); [Noordhui et al., 2008](#); [Chang et al., 2015](#); [Wei et al., 2014](#), [Sönmez M. et al., 2010](#)). The presence of metal centers capable of binding to negatively charged bio-ligands, as proteins and nucleic acids offers the metal complexes excellent potential pharmaceutical properties ([Sakurai et al., 2002](#); [Jian et al., 2010](#)). The metal complex is considered a chemotherapeutic agent in cancer treatment, when it slows and stops the cancer from spreading by killing the rapidly

35 dividing cells. In chemotherapy, the target is to kill the tumor cells, without causing damage to the  
36 healthy cells. Cisplatin and carboplatin have been used in the treatment of various cancers as  
37 chemotherapeutic agents (Kostova, 2006). Serious side effects accompany the use of these drugs,  
38 so, trials are done to find new platinum complexes with less toxicity, to be used as potential anti-  
39 cancer agents (Ehrsson et al., 2002). As a result, new platinum complexes with different organic  
40 ligands have been designed (Al Jibori et al., 2014; Tabrizi and Chiniforoshan, 2017., Wang et al.,  
41 2015; Wang et al., 2017).

42 In this paper a new Pt(II) complex of a hydrazide derivative N-(5-indanyl(methylene)anthranilic  
43 acid (5-indanyl methylene)-hydrazide has been synthesized and characterized by various  
44 techniques. The cytotoxic effect of the synthesized Pt(II) complex was studied.

45 To the best of our knowledge no work has been carried out on the present ligand, only a patent  
46 described the synthesis, the anti-inflammatory and analgesic activity of similar derivatives  
47 N-(substituted-naphthyl-1) anthranilic acid, was presented (Fujio and Tomoaki 1976).

## 48 **Materials and methods**

49 N-(5-indanyl(methylene)anthranilic acid(5-indanyl methylene)-hydrazide and PtCl<sub>2</sub> were  
50 purchased from Sigma-Aldrich (S512095). <sup>1</sup>H-NMR of the ligand in DMSO-*d*<sub>6</sub> δ (ppm): 2.0 (m,  
51 2H, CH<sub>3</sub>), 2.49 (t, 4H, C<sub>5</sub>-2H), 2.8 (t, 2H, 2H). CH=N appears at 6.8 (s, 1H), 7.43-7.8 (m, 10H).

## 52 **Instruments**

53 The elemental analysis, C, H and N were carried in the instrumentation center, Granada University,  
54 Spain, on Thermo Scientific Flash 2000 Analyzer. TGA (thermo-gravimetric analysis  
55 measurements) were carried out on a Shimadzu model 50 H instrument with nitrogen flow rate 20  
56 cm<sup>3</sup>/min., and heating rate 10 °C/min. Magnetic measurements were carried out on a Sherwood  
57 Scientific Magnetic Balance. The <sup>1</sup>H-NMR spectra in DMSO-*d*<sub>6</sub> were carried out on a 500 MHz  
58 JEOL spectrophotometer. Fourier-transformer infrared spectra (FT-IR) were carried out as KBr  
59 discs on a Mattson 5000 FTIR spectrometer. EI-MS was recorded on spectrometer WATERS  
60 modelo SYNAP G2 in instrumentation center, Granada University, Spain. CM 20 PHILIPS electron  
61 microscope was used to take the transmittance electron microscope (TEM) images.

## 62 **Synthesis of Pt(II) complex**

63 0.001 M (0.265 gm) of PtCl<sub>2</sub> in 10 ml ethanol was injected to 0.001 M (0.40 gm) of (N-(5-  
64 indanyl(methylene)anthranilic acid (5-indanyl methylene)-hydrazide in 25 ml hot ethanolic solution  
65 under nitrogen. A yellow precipitate was formed on reflux. The reaction mixture was refluxed for 3  
66 hrs and the precipitate was filtered off under vacuum.

67 The trials to obtain a single crystal from the platinum complex was failed.

68 Yellow powder (yield 55%); m.p. >300 °C. Anal. Calc. for PtC<sub>54</sub>H<sub>57</sub>N<sub>6</sub>O<sub>6.5</sub>: C, 59.6; H, 5.3; N, 7.7;  
69 Pt, 17.9% Found: C, 60.0; H, 5.4; N, 7.3; Pt, 18.1 %.

## 70 **Pharmacological testing**

### 71 *In vitro study (Cytotoxicity)*

72 Cytotoxic activity of Pt(II) was performed on a panel of human tumor cell line HEPG2  
73 (hepatocellular carcinoma), HCT 116 ( human colon cancer) at different concentrations. The  
74 method of Philp et al was used to carry out the cytotoxicity as sulphorhodamine-B(SRB) assay  
75 (Philips *et al.*, 1990). SRB is a protein stain in mild acidic conditions. This stain is used to provide a  
76 sensitive index of cellular protein content. It is a bright pink amnoxanthrene dye with two  
77 sulphonic groups.

### 78 *In vivo study (Toxicity studies)*

79 LD50 of Pt(II) complex in mice was determined according to the method of Meier and Theakston  
80 (Meier and Theakston 1986).

### 81 *Dose response*

82 Dose response of Pt(II) complex was determined in mice according to the method described by  
83 Crump et al (Crump *et al.*, 1976). Animal care and experiments were performed in accordance with  
84 NIH guide to the care and use of laboratory animals.

85 Experimental design: 20 female Swiss albino mice were divided into two groups (10 mice per each  
86 group): Group I is the positive control and injected intraperitoneally with 2.5x10<sup>6</sup> of Ehrlich ascites  
87 carcinoma "EAC" cells. Group II is the Pt(II) complex therapeutic group, injected intraperitoneally  
88 with 2.5x10<sup>6</sup> of Ehrlich ascites carcinoma "EAC" cells, and after one day of EAC injection,  
89 therapeutic group injected intraperitoneally with 5 mg/kg of Pt(II) complex day after day. At the end  
90 of the experiment, EAC cells were collected from mice and viability study was assayed.

### 91 *Cell viability and counting of EAC cells*

92 Trypan blue exclusion method (McLiman *et al.*, 1957) was used to determine the counting and  
93 viability of EAC cells. The total and viable cells (nonstained) were determined in the two groups as  
94 the number of cells /ml at magnification power X40.

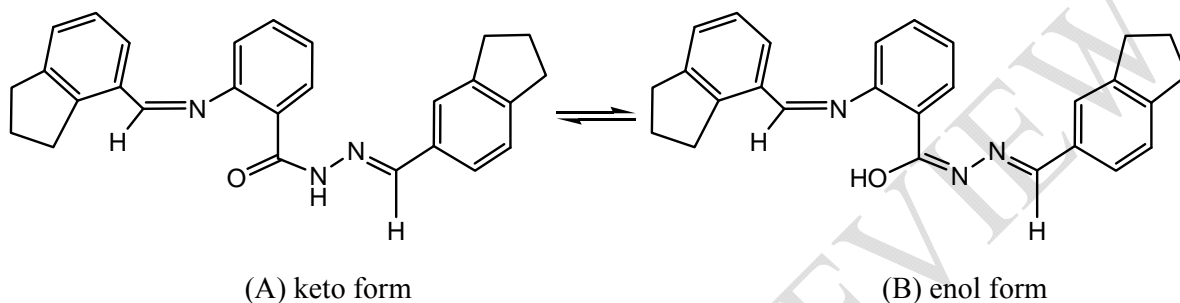
### 95 **Statistical analysis**

96 SPSS software version 14 (Levesquie 2007) was used to perform statistical analysis. One way  
97 analysis of variance was used to assess using the effect of each parameter. The results were  
98 presented as mean ± SD. Analysis of variance (ANOVA test), was used to determine the differences  
99 between mean values followed by Duncan's multiple rank test using MSTAT-C computer program.  
100 From linear regression analysis the statistical significance (where P ≤ 0.05 was considered  
101 significant) of the relationships between variables was calculated.

## 102 Results and discussion

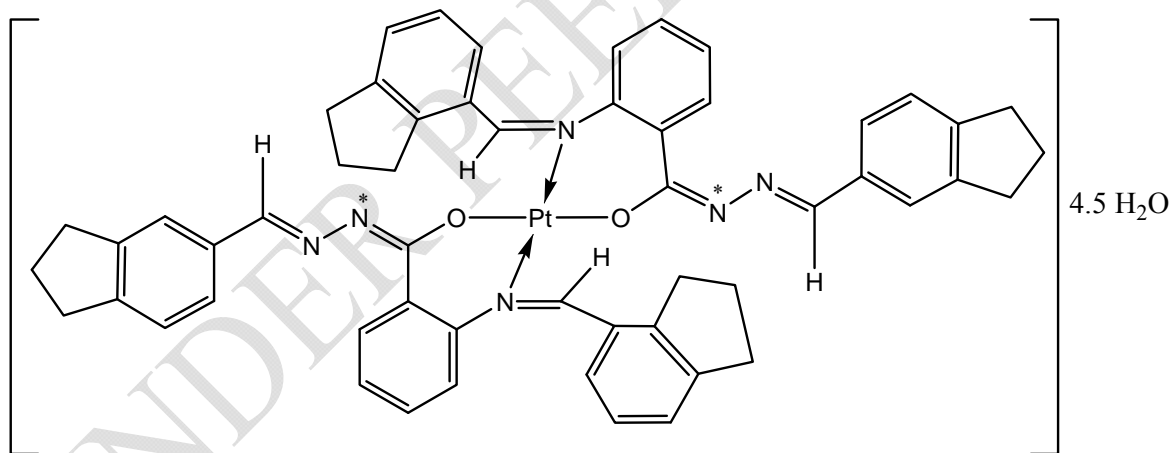
### 103 IR spectra of the ligand and its Pt(II) complex

104 Two tautomeric forms are suggested for the ligand, the Keto (Fig.1 A) and the enol (Fig.1B). The  
105 keto form (1A) is the major tautomer in the solid state. The formula  $[Pt(L)_2] \cdot 4.5H_2O$  represents the  
106 complex formed from the reaction of (N-(5-indanyl(methylene)anthranilic acid (5-indanyl  
107 methylene)-hydrazide and  $PtCl_2$ . The ligand chelates the Pt(II) ion in the enol form after  
108 displacement of hydrogen ion from the enolic carbonyl (Fig. 2).



109  
110 Fig.1. The two possible tautomeric forms of the ligand.

111 The isolated Pt(II) complex is stable in air, soluble in coordinating solvents as DMF and  
112 DMSO, but insoluble in water. The elemental analysis indicated that the isolated Pt(II) complex is  
113 pure compound.



114  
115 Fig. 2. Suggested structure of Pt(II) complex

116 Some important IR bands of the ligand and its Pt(II) complex with their probable  
117 assignments are indicated in Table 1. The ligand exhibits strong band at  $3286\text{ cm}^{-1}$  due to  $\nu$  (NH).  
118 The strong bands at  $1662$  and  $1621\text{ cm}^{-1}$  are attributed to  $\nu$  (C=O) and  $\nu$  (CONH), respectively  
119 (Nakamoto, 1970; Hosny and Sherif 2015; Hosny (2009); Hosny and Shallaby (2007). These bands  
120 confirm the presence of the free ligand in the keto form. The ligand shows also, bands at  $1605$ ,  
121  $1306$ ,  $1199$  and  $971\text{ cm}^{-1}$  attributed to  $\nu$  (HC=N),  $\nu$  (C-O),  $\nu$  (C-N) and  $\nu$  (N-N), respectively  
122 (Nakamoto, 1970; Hosny, 2010). Comparison of the IR spectrum of the ligand with that of Pt(II)

123 complex reveals that the ligand chelates Pt(II) ion in a mono-negative bidentate mode *via*  
 124 azomethine nitrogen (C=N) and the enolized carbonyl oxygen after displacement of hydrogen (Fig.  
 125 2). The disappearance of the strong bands assigned to  $\nu(\text{NH})$ ,  $\nu(\text{CO})$  and  $\nu(\text{CONH})$  in the free  
 126 ligand and the appearance of a new medium band at  $1650\text{ cm}^{-1}$  assigned to  $\nu(\text{C}=\text{N}^*)$  in the spectrum  
 127 of Pt(II) complex support the suggested chelation mode. There is other possible coordination mode  
 128 which may exist for the ligand, including formation of 5-membered chelate ring through N-N=CH  
 129 group. This latter mode was discarded on the basis of the remaining of the bands at  $969$  and  $1605$   
 130  $\text{cm}^{-1}$  due to  $\nu(\text{N-N})$  and  $\nu(\text{HC}=\text{N})$  unaltered in comparison with its position in the spectrum of the  
 131 organic ligand. The remaining of these bands unaltered, confirms the inertness of N-N active sites  
 132 towards coordination (Nakamoto, 1970). The presence of hydrated water in the Pt(II) complex is  
 133 confirmed by the presence of bands at  $3431$ ,  $746$  and  $690\text{ cm}^{-1}$  due to  $\nu(\text{OH})$ ,  $\delta(\text{OH})$  and  $\rho_w(\text{OH})$ ,  
 134 respectively (Misbahur Rehman, 2017; Hussien et al., 2015; Hosny et al., 2014). New weak bands  
 135 are observed at  $557$  and  $449\text{ cm}^{-1}$  due to  $\nu(\text{M-O})$ ,  $\nu(\text{M-N})$  respectively (Hosny 2007; Sherif and  
 136 Hosny, 2014).

137 **Table1.** IR spectral data in ( $\text{cm}^{-1}$ ) for the ligand (HL) and its Pt(II) complex.

Compound	$\nu(\text{NH})$	$\nu(\text{C}=\text{O})$	$\nu(\text{C}=\text{N}^*)$	$\nu(\text{C}=\text{N})$	$\nu(\text{C-O})$	$\nu(\text{C-N})$	$\nu(\text{M-O})$	$\nu(\text{M-N})$
The ligand (HL)*	3286	1662	-	1605	1306	1199	-	-
[Pt(L) <sub>2</sub> ] <sub>3</sub> H <sub>2</sub> O	-	-	1650	1603	1292	1144	557	445

138 \* HL = (N-(5-indanyl(methylene)anthranilic acid (5-indanyl methylene)-hydrazide

139 Pt(II) complex may exist either in N-N (*cis*), O-O(*cis*) or N-N(*trans*),O-O (*trans*). Molecular  
 140 mechanics method was used to predict rapidly the geometries of the two suggested conformers by  
 141 using hyperchem series of programs (Hyperchem 7, 2002). The total energy calculations of the two  
 142 structures indicated that the *trans* form is only  $2\text{ KJ mol}^{-1}$  more stable than the *cis* form.

### 143 <sup>1</sup>H-NMR

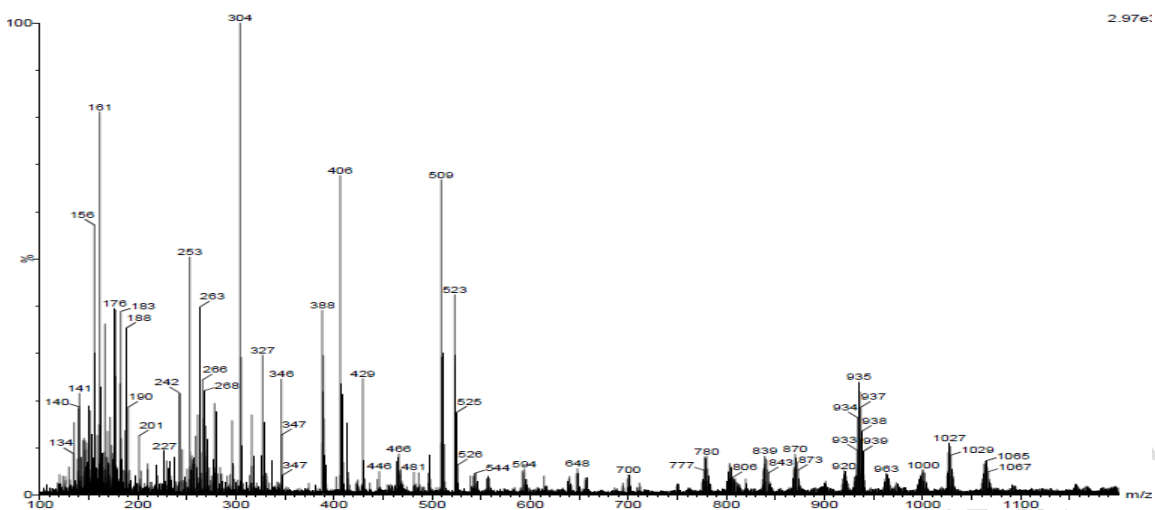
144 <sup>1</sup>H-NMR spectrum of the ligand (N-(5-indanyl(methylene)anthranilic acid (5-indanyl methylene)-  
 145 hydrazide in DMSO-d<sub>6</sub> shows signals attributed to cyclopentane ring at  $\delta$  1.92-1.99 (m, 4H, 2CH<sub>2</sub>)  
 146 and 2.75-2.86 (m, 16H, 6CH<sub>2</sub>, 4CH ) (Dezső et al; 2001). Three singlet signals appear at  $\delta$  6.42,  
 147 7.55, 8.73 ppm due to the protons of secondary amine NH and two azomethine protons (CH=N) and  
 148 CH=N-NH, respectively (Gołębiewski and Cholewińska 2004). The multiplet signals integrated for  
 149 6 protons resonate around 6.75 and 7.29-7.54 ppm characteristic for cyclohexadiene olefinic

150 protons. The four aromatic protons of the benzene ring are observed in the region 7.13-7.27(m, 2H,  
151 Ar-H) and (m, 2H, Ar-H) (Gołębiewski and Cholewińska 2004).

152 <sup>1</sup>H-NMR spectrum of Pt(II) complex taken in DMSO-d<sub>6</sub> reveals beside the expected signals  
153 of cyclopentane ring, cyclohexadiene olefinic protons in the range 1.99-3.80 ppm and the aromatic  
154 protons in 6.70-7.50 ppm. The absence of the NH signal which appears at δ 6.42 ppm in the  
155 spectrum of the free ligand was attributed to the enolization of the carbonyl with subsequent  
156 liberation of this proton on coordination to the Pt(II) ion. The singlet signal of the azomethine  
157 (CH=N) resonates downfield at δ 8.00 ppm. This shift in the signal position supports the  
158 participation of the azomethine group in complex formation.

### 159 **Mass spectra**

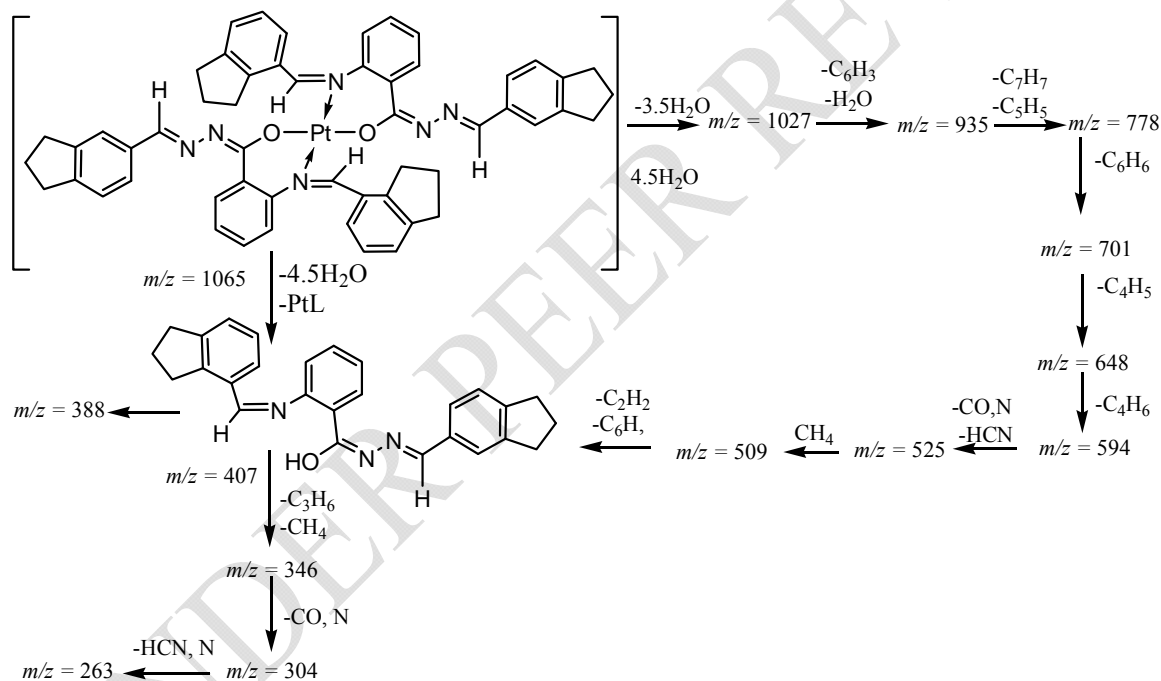
160 The EI-MS of Pt(II) complex (Fig. 3) exhibits the molecular ion peak at  $m/z = 1087$ , in agreement  
161 with the formula [Pt(C<sub>27</sub>H<sub>23</sub>N<sub>3</sub>O)<sub>2</sub>]<sub>4.5</sub>H<sub>2</sub>O after removal of H<sub>2</sub>. Two possible pathways have been  
162 suggested for the fragmentation of Pt(II) complex (Scheme 1). The molecular ion peak may lose  
163 four and half water molecules and the fragment [PtL] to give a peak at  $m/z = 406$ , assigned to the  
164 free ligand. The free ligand is fragmented by loss of propene and methane molecule by special  
165 rearrangement to give the peak at  $m/z = 346$ . The last peak is further fragmented by loss of carbon  
166 monoxide and nitrogen giving the base peak at  $m/z = 304$ . The base peak loses hydrocyanic acid and  
167 nitrogen forming the peak at  $m/z = 263$ . In the second pathway, it was suggested that the molecular  
168 ion peak loses three and half molecules of water forming the peak at  $m/z = 1027$ . The latter peak is  
169 fragmented by lose of water molecule and the fragment C<sub>6</sub>H<sub>3</sub> giving the peak at  
170  $m/z = 935$ . The latter peak loses tropyllium and furayl groups to give the peak at  $m/z = 778$ . The  
171 peak at  $m/z = 778$  is further fragmented by loss of benzene and butadiene to give the peaks at  $m/z =$   
172 701 and 648, respectively. The last fragment loses butane to produce the fragment at  $m/z = 594$ ,  
173 which loses hydrocyanic acid, carbon monoxide and nitrogen producing the fragment  $m/z = 525$ .  
174 The last fragment at  $m/z = 525$  loses methane, ethylene and benzene leading to the peak corresponds  
175 to the free ligand at  $m/z = 407$ .



176

177 Fig. 3 . MS of Pt(II) complex

178



179

180 Scheme 1. Fragmentation pattern of Pt(II) complex

### 181 Magnetic measurements

182 The Pt(II) complex is diamagnetic which confirms the formation of a square–planar stereochemistry  
 183 around the Pt(II) ion (Lever, 2002).

### 184 Thermal analysis

185 TGA measurements of Pt(II) complex were carried out from 25 °C up to 1000 °C.  
 186 The thermogram exhibits three events. The first resulted from the removal of water of hydration.  
 187 This step starts from 25 °C to 140 °C (Soliman et al 2005). The next step was attributed to the loss

188 of two phenyl and four benzocyclopentane rings. This step takes place from 141 °C to 480 °C.  
189 (Found mass loss of this step is 55.5%, while the calculated mass loss is 57.0%). The last step starts  
190 from 461 °C to 880 °C, corresponding to the loss four hydrocyanic acid molecules (Found mass loss  
191 of this step is 8.7%; Calcd 9.0%).

192 The thermodynamic parameters of decomposition were calculated by applying Coats-Redfern  
193 (Coats-Redfern, 1964) equations. The energy of activation ( $E^*$ ) and the order of the reaction ( $n$ )  
194 were determined graphically. The thermodynamic parameters  $E^*$ ,  $\Delta H^*$ ,  $\Delta G^*$  and  $\Delta S^*$  were calculated  
195 from equations (1-3) and found to be 10.5, 4.7, 217 KJ and  $-301.7 \text{ S}^{-1}$ , respectively:

$$196 \quad \Delta S^* = 2.303 [\log (Zh/KT)]R \quad (1)$$

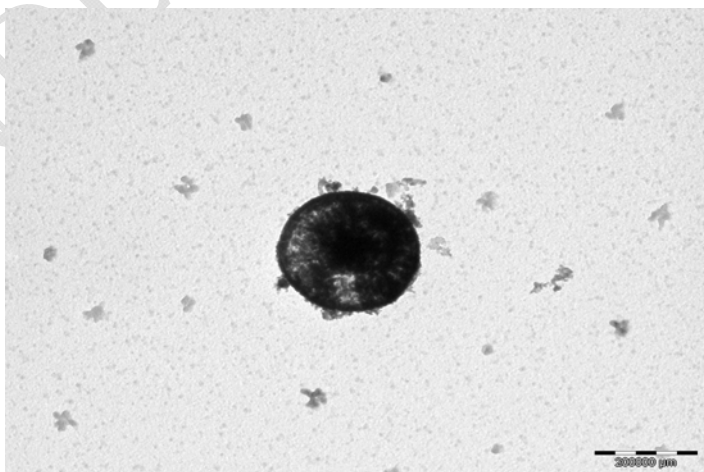
$$197 \quad \Delta H^* = E - RT \quad (2)$$

$$198 \quad \Delta G^* = \Delta H^* - Ts \Delta S^* \quad (3)$$

199 (Where,  $Z$ ,  $h$  and  $K$  are the pre-exponential factor, Plank and Boltzmann constants, respectively  
200 (Sherif and Hosny, 2014). The thermodynamic parameters were calculated for the second step,  
201 which is suitable for kinetic analysis, where there is no overlapping with other steps. The positive  
202 enthalpy and free energy values reveal the endothermic and non-spontaneous decomposition of this  
203 step, respectively. The negative entropy value indicates that the structure of the activated complex is  
204 more ordered than the reactants (Sherif and Hosny, 2014).

#### 205 **Morphological characterization**

206 The chemical and biological activities of metal complexes were related to their particles size and  
207 shape (Hussain and Chakravrti,2012; Hosny et al., 2015). Transmittance electron microscope  
208 (TEM) was used to determine the particles shape and size of Pt(II) complex. From the TEM images  
209 (Fig.4), it is clear that the particles of Pt(II) complex are spherical in shape.



219

Fig. 4. TEM images of Pt(II) complex



220 The possible formation mechanism of the spherical particles of Pt(Indanyl) complex has been  
 221 proposed as indicated in Scheme 1. Under reflux conditions, the soluble Pt<sup>2+</sup> cation reacts with the  
 222 indanyl ligand to form insoluble Pt(Indanyl) nucleus. In the first stage, Pt(Indanyl) complex follows  
 223 a heterogeneous nucleation, where the energy barrier is lower than nucleation in solution (Luo et al.,  
 224 2011; Mohammadikish 2014). Initially, large numbers of small primary nanoparticles are formed.  
 225 These primary particles have high surface energy, which makes them unstable. They aggregate  
 226 rapidly and grow forming spherical nanoparticles. The nanospheres are assembled to each other via  
 227 random attachment to reduce the surface energy forming thermodynamically stable structure.  
 228 Finally, spontaneous aggregation takes place in spherical form to minimize the surface area.

## 229 Biological Study

### 230 Cytotoxicity

231 The in vitro cytotoxic activities of Pt(II) and the standard doxorubicin were shown in Table 2 and  
 232 Figs 5, 6. The minimum inhibitory concentration of the synthesized compound was found to be 5.3  
 233 µg/ml and 9.68 µg/ml against HCT116 and HEPG2 cell lines, respectively. The colorimetric  
 234 cytotoxicity tests showed that the Pt(II) complex has in vitro cytotoxic activity against the examined  
 235 cancerous cell lines with IC<sub>50</sub> values of 9.08 µM and 5.43 µM against HCT116 and HEPG2 cell  
 236 lines, respectively. The current results revealed that the present Pt complex inhibits cell proliferation  
 237 in the same range as cisplatin and oxaliplatin.

238 **Table 2.** Minimum inhibitory concentration of doxorubicin and synthesized Pt(II) complex against  
 239 HCT116 and HEPG2 cell lines

	HCT116	HEPG2
Doxorubicin	5.3 µg/ml	5.18 µg/ml
Pt (II) complex	9.68 µg/ml	5.78 µg/ml

240

### 241 Determination of median lethal dose (LD50) of Pt(II) complex

242 The results revealed that, dose up to 100 mg/kg body weight was considered safe, where no  
 243 mortality was observed. Table 3 summarizes the effect of Pt(II) complex on EAC cells volume and  
 244 count.

245

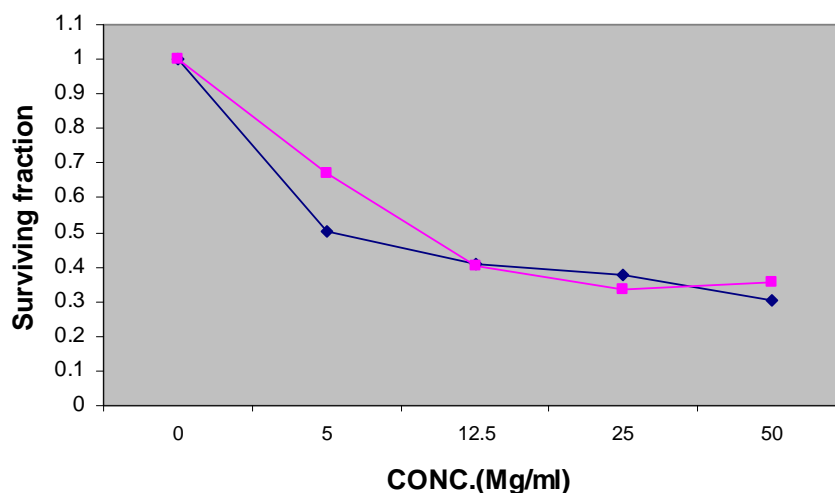
246 **Table 3.** Effect of Pt (II) complex on the volume and count of EAC in the studied groups:

Parameter	Positive control	Pt(II) complex
Volume of Ascites fluid(ml)	3.9 ± 0.11	2.24±0.18

% change	-	42.56%
Count of EAC cells ( $\times 10^6$ )	$55.4 \pm 0.32$	$26.3 \pm 0.64$
% change	-	52.53%

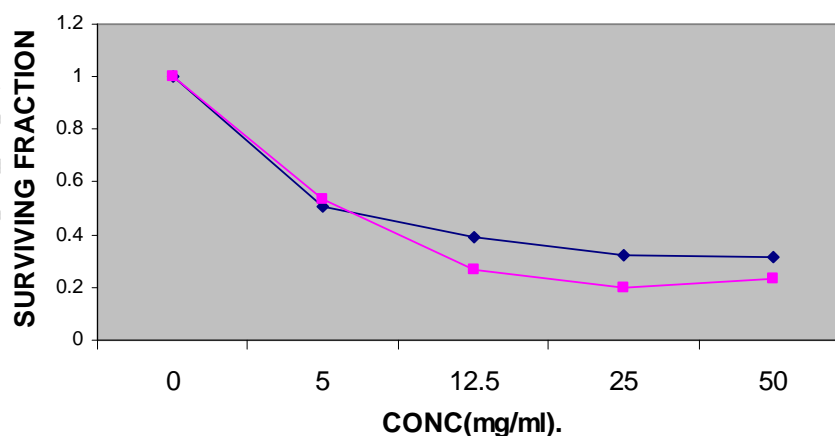
247

248 The results indicate mean volume of EAC of the positive control group is 3.9 ml. This value was  
 249 significantly decreased by 42.5% in Pt(II) complex treated group ( $P < 0.05$ ). Also, it was found that  
 250 the mean count of EAC cells in the positive control group is  $55.4 \times 10^6$  which was significantly  
 251 decreased in Pt(II) complex treated group, compared to the positive control group.



252

253 Fig. 5. Minimum inhibitory concentration of Pt(II) complex (pink) and doxorubicin (blue) against  
 254 HCT cell line



255

256 Fig. 6. Minimum inhibitory concentration of Pt(II) complex (pink) and doxorubicin (blue) against  
 257 HEPG2T cell line

258 **Conclusion**

259 To the best of our knowledge no work has been carried out on the ligand  
260 N-(5-indanyl(methylene)anthranilic acid(5-indanyl methylene)-hydrazide and its metal complexes.  
261 The Pt(II) complex of this ligand has been synthesized and characterized by different techniques.  
262 The ligand coordinates to the Pt(II) ion in the enol form as mono-negative bidentate forming  
263 square-planar complex. TEM images indicated that the particles of Pt(II) complex exist as spherical  
264 nanoparticles. The Pt(II) complex exhibits activities on four human cancer cell lines HEPG2  
265 and HCT 116 with  $IC_{50} = 1.4-9.6 \mu M$ . The activity of the Pt(II) complex was compared with some  
266 standard platinum complexes as cisplatin and carboplatin complexes.

267  
268 **References**

269 **Al-Jibori S. A.**, Al-Jibori G. H., Al-Hayaly L. J., Wagner C., Schmidt H., Timur S., Barlas F. B.,  
270 Subasi E., Ghosh S., Hogarth G. 2014. Combining anti-cancer drugs with artificial sweeteners:  
271 Synthesis and anti-cancer activity of saccharinate (sac) and thiosaccharinate (tsac) complexes *cis*-  
272 [Pt(sac)<sub>2</sub>(NH<sub>3</sub>)<sub>2</sub>] and *cis*-[Pt(tsac)<sub>2</sub>(NH<sub>3</sub>)<sub>2</sub>], *Journal of Inorganic Biochemistry*, 141: 55.  
273 [doi:10.1016/j.jinorgbio.2014.07.017](https://doi.org/10.1016/j.jinorgbio.2014.07.017)

274 **Coats A. W.**, Redfern J. P. (1964) Kinetic parameters from thermogravimetric. *Nature*, 201:68.  
275 [doi:10.1038/201068a0](https://doi.org/10.1038/201068a0)

276 **Crump K. S.**, Hoel D. G., Langley C. H., Peto R. 1976. Fundamental carcinogenic processes and  
277 their implications for low dose risk assessment. *Cancer Research*, 36:2973.  
278 [doi: Published September 1976](https://doi.org/10.1056/NEJM197609133618)

279 **Dezső G.**, Evanics F., Dombi G., Bernáth G. 2001. <sup>1</sup>H and <sup>13</sup>C NMR Chemical shift assignments of  
280 a cyclopentane-fused *cis*-azetidinone (*cis*-azabicyclo[3.2.0]heptan-7-one). *Atheoretical and*  
281 *experimental investigation. ARKIVOC III: 73.*

282 **Divsalar A.**, Zhila I., Saboury A. A., Nabiuni M., Razmi M., Mansuri-Torshizi H. 2013. Cytotoxic  
283 and spectroscopic studies on binding of a new synthesized bipyridine ethyl dithiocarbamate Pt(II)  
284 nitrate complex to the milk carrier protein of BLG. *Journal of Iranian Chemical Society*, 10: 951.  
285 DOI 10.1007/s13738-013-0232-6

286 **Ehrsson H.**, Wallin I., Yachnin J. 2002. Pharmacokinetics of oxaliplatin in humans. *Medical*  
287 *Oncology*, 16: 261. [doi:10.1385/MO:19:4:261](https://doi.org/10.1385/MO:19:4:261)

- 288 **Foltinova V.**, Svihalkova L. S., Horvath V., Sova P., Hofmanova J., Janisch R., Kozubík A. 2008.  
289 Mechanism of effects of Pt(II) and (IV) complexes. Comparison of cis platin and oxaliplatin with  
290 satraplatin and LA-12, new platinum (IV) based drugs. A mini review. *Scripta Medica (BRNO)*,  
291 81:105.
- 292 **Fujio N.**, Tomoaki F. 1976. Substituted naphthyl anthranilic acids. *United States Patents*,  
293 3989746A.
- 294 **Golebiewski M.**, Cholewińska M. 2004. Synthesis and spectral studies of transition metal  
295 complexes of aryloylhydrazones of 5- methylsalicylaldehyde, *Pestycydy*, 1-2: 21.
- 296 **Grunicke H.**, Doppler W., Helliger W. 1986. Tumor biochemistry as basis for advances in tumor  
297 chemotherapy. *Archive Geschwulstforsch*, 156:193. [PMID:3488047](#)
- 298 **Hosny N. M.** 2007. Synthesis, characterization, theoretical calculations and catalase-like activity of  
299 mixed ligand complexes derived from alanine and 2-acetylpyridine. *Transition Metal Chemistry*,  
300 32: 117. [doi: 10.1007/s11243-006-0132-z](#)
- 301 **Hosny N. M.** 2009. Synthesis and Characterization of Transition Metal Complexes Derived from  
302 (E)-(N)-(1-(Pyridine-2-yl)ethylidene)benzohydrazide (PEBH). *Journal Molecular Structure*,  
303 923:98. [doi.org/10.1080/15533174.2011.591296](#)
- 304 **Hosny N. M.** 2010. Cu(II) and Zr(IV) Complexes with (E)-N-(1-(Pyridine-4-  
305 yl)ethylidene)nicotinohydrazide. *Synth. React. Inorg-Org Met Nano* 6: 391.  
306 [doi:10.1080/15533174.2010.492550](#)
- 307 **Hosny N. M.**, El Morsy E. A., Sherif Y. E. 2015. Synthesis, spectral, optical and anti-inflammatory  
308 activity of complexes derived from 2-aminobenzohydrazide with some rare earths.  
309 *Journal of Rare Earths*, 33: 758. [doi.org/10.1016/S1002-0721\(14\)60482-8](#)
- 310 **Hosny N. M.**, Hussien M. A., Radwan F. M., Nawar N. 2014. Synthesis, spectral characterization  
311 and DNA binding of Schiff-base metal complexes derived from 2-amino-3-hydroxypropanoic acid  
312 and acetylacetone. *Spectrochimica Acta A*, 132: 121. [doi:10.1016/j.saa.2014.04.165](#)
- 313 **Hosny N. M.**, Shallaby A. M. 2007. Spectroscopic Characterization of Some Metal Complexes  
314 Derived from 4-Acetylpyridine Nicotinoylhydrazone, *Transition Metal Chemistry*, 32:1085. [Doi: 10.1007/s11243-007-0288-1](#)
- 315  
316 **Hosny N. M.**, **Sherif Y. E.** 2015. Synthesis, structural, optical and anti-rheumatic activity of  
317 metal complexes derived from (E)-2-amino-N-(1-(2-aminophenyl)ethylidene) benzohydrazide (2-

318 AAB) with Ru(III), Pd(II) and Zr(IV). *Spectrochimica Acta A*, 136:510.  
319 [doi.org/10.1016/j.saa.2014.09.064](https://doi.org/10.1016/j.saa.2014.09.064)

320 **Hussain J., Chakravarty A. R.** 2012. Photocytotoxic lanthanide complexes, *Journal of Chemical*  
321 *Science*, 124:1327.

322 **Hussien M. A., Nawar N., Radwan F. M., Hosny N. M.** 2015. Spectral characterization, optical  
323 band gap calculations and DNA binding of some binuclear Schiff-base metal complexes derived  
324 from 2-amino-ethanoic acid and acetylacetonate, *J. Mol. Struct.*, 1080:162.  
325 [doi.org/10.1016/j.molstruc.2014.09.071](https://doi.org/10.1016/j.molstruc.2014.09.071)

326 **Hyperchem 7**, developed by Hypercube Inc. 2002.

327 **Jain A., Jain S. K., Ganesh N.** 2010. Design and development of ligand-appended polysaccharidic  
328 nanoparticles for the delivery of oxaliplatin in colorectal cancer, *Nanomedicine Nanotechnology*  
329 *Biology and Medicine*, 6: 179. DOI:[10.1016/j.nano.2009.03.002](https://doi.org/10.1016/j.nano.2009.03.002)

330 **Kostova I.** 2006. Platinum complexes as anticancer agents, *Recent Patents on Anti-Cancer Drug*  
331 *Discovery*, 1:1.

332 **Lever A. B. P.** 1986. Inorganic electronic spectroscopy, Elsevier, Amsterdam.

333 **Levesque R.** 2007. SPSS: Programming and Data Management: A Guide for SPSS and SAS users,  
334 Fourth Edition, SPSS INC , Chicago III.

335 **Luo L. J.,** Tao W., Hu X. Y., Xiao T., Heng B. J., Huang W., Wang H., Han H. W., Jiang Q. K.,  
336 Wang J. B., Tan Y. W. 2011. Mesoporous F-doped ZnO prism arrays with significantly enhanced  
337 photovoltaic performance for dye-sensitized solar cells. *Journal of Power Sources*, 196: 10518.  
338 [doi.org/10.1016/j.jpowsour.2011.08.011](https://doi.org/10.1016/j.jpowsour.2011.08.011)

339 **McLiman W. F.,** Dairs E. V., Glover F. L., Rake G. W. 1957. The submerged culture of mammalian  
340 cells; the spinner culture, *Journal of Immunology*, 79:428. PMID:[13491853](https://pubmed.ncbi.nlm.nih.gov/13491853/)

341 **Meier J.,** Theakston R. D. 1986. Approximate LD50 determinations of snake venoms using eight to  
342 ten experimental animals. *Toxicology Journal*, 24:395. PMID:[3715904](https://pubmed.ncbi.nlm.nih.gov/3715904/)

343 **Misbah ur Rehman,** Imran M., Arif M. 2013. Synthesis, Characterization and in vitro  
344 Antimicrobial studies of Schiff-bases derived from Acetylacetonate and amino acids and their  
345 oxovanadium(IV) complexes. *American Journal of Applied Chemistry*, 1: 59. doi:  
346 [10.11648/j.ajac.20130104.13](https://doi.org/10.11648/j.ajac.20130104.13)

347 **Mohammadikish M.** 2014. Green synthesis and growth mechanism of new nanomaterial: Zn  
348 (salen) nano-complex. *Crystal Engineering Communication*,  
349 16:8020.[doi.org/10.1016/j.jcrysgro.2015.08.029](https://doi.org/10.1016/j.jcrysgro.2015.08.029)

350 **Mujahid M.,** Kia A. F., Duff B., Egan D. A., Devereux M., McClean S., Walsh M., Trendafilova  
351 N., Georgieva I., Creaven B. S. 2015. Spectroscopic studies, DFT calculations, and cytotoxic  
352 activity of novel silver(I) complexes of hydroxy ortho-substituted-nitro-2H-chromen-2-one ligands  
353 and a phenanthroline adduct. *Journal Inorganic*  
354 *Biochemistry*,153:103.[doi:10.1016/j.jinorgbio.2015.10.007](https://doi.org/10.1016/j.jinorgbio.2015.10.007)

355 **Nakamoto K.,** (ed). (1970) Infrared spectra of inorganic and coordination compounds. John Wiley,  
356 New York.

357 **Noordhui P.,** Laan A., Born K., Losekoot N., Kathmann I., Peters G. 2008. Oxaliplatin activity in  
358 selected and unselected human ovarian and colorectal cancer cell lines. *Biochemical Pharmacol*  
359 *ogy*, 76: 53. [doi:10.1016/j.bcp.2008.04.007](https://doi.org/10.1016/j.bcp.2008.04.007)

360

361 **Philips S.,** Rista S., Dominic S., Anne M., Jaames M., David V., Jonathan T. W., Heidi B., Susan  
362 K., Michael R. B. 1990. Newcoloremtric cytotoxicity assay for anti-cancer drug screening. *Journal*  
363 *of National Cancer Institute*, 8:1107. [doi:10.1016/j.bcp.2008.04.007](https://doi.org/10.1016/j.bcp.2008.04.007)

364 **Sakurai H.,** Kojima Y., Yoshikawa Y., Kawabe K., Yasui H. 2002. Antidiabetic vanadium(IV) and  
365 zinc(II) complexes. *Coordination Chemistry Review*, 226: 187. [doi.org/10.1016/S0010-](https://doi.org/10.1016/S0010-8545(01)00447-7)  
366 [8545\(01\)00447-7](https://doi.org/10.1016/S0010-8545(01)00447-7)

367 **Sherif Y. E.,** Hosny N. M. 2014. Synthesis, characterization, and anti-rheumatic potential of  
368 phthalazine-1,4-dione and its Cu(II) and Zn(II) complexes, *Medicinal Chemistry Research*,  
369 23:2536. [doi: 10.1007/s00044-013-0827-6](https://doi.org/10.1007/s00044-013-0827-6)

370 **Sherif Y. E.,** Hosny N. M. 2014. Anti-rheumatic potential of ethyl 2-(2-cyano-3-mercapto-3-  
371 (phenylamino) acrylamido)-4,5,6,7-tetrahydrobenzo[b]thiophene-3-carboxylate and its Co(II),  
372 Cu(II) and Zn(II) complexes, *European Journal of Medicinal Chemistry*, 83: 338.  
373 [doi.org/10.1016/j.ejmech.2014.06.038](https://doi.org/10.1016/j.ejmech.2014.06.038)

374 **Soliman A. A.,** Mohamed G. G., Hosny W. M., El-Mawgood M. A. 2005. Synthesis,  
375 Spectroscopic and thermal characterization of new sulfasalazine metal complexes. *Synth. React.*  
376 *Inorg. Met-Org. Nano-Met.Chem.* , 35:483. DOI: [10.1081/SIM-200067043](https://doi.org/10.1081/SIM-200067043)

377

- 378 **Sönmez M.**, Celebi M., Yardim Y., Sentürk Z. 2010. Palladium(II) and platinum(II) complexes a  
379 symmetric Schiff base derived from 2,6-diformyl-4-methylphenol with N-aminopyrimidine:  
380 Synthesis, characterization and detection of DNA interaction by voltammetry, *European Journal of*  
381 *Medicinal Chemistry*, 45: 4215. doi: [10.1016/j.ejmech.2010.06.016](https://doi.org/10.1016/j.ejmech.2010.06.016).
- 382 **Tabrizi L.**, Chiniforoshan H. 2017. Cytotoxicity and cellular response mechanisms of water-  
383 soluble platinum(II) complexes of lidocaine and phenylcyanamide derivatives. *BioMetals*,  
384 30:59. doi:[10.1007/s10534-016-9986-5](https://doi.org/10.1007/s10534-016-9986-5)
- 385 **Wang B.**, Wang Z., Ai F., Tang W. K., Zhu G. 2015. A monofunctional platinum(II)-based  
386 anticancer agent from a salicylanilide derivative: Synthesis, antiproliferative activity, and  
387 transcription inhibition, *Journal of Inorganic Biochemistry*. 142: 118.  
388 [doi.org/10.1016/j.jinorgbio.2014.10.003](https://doi.org/10.1016/j.jinorgbio.2014.10.003)
- 389 **Wang Q.**, Yang L., Wu J., Wang H., Song J., Tang. X. 2017. Four mononuclear platinum(II)  
390 complexes: Synthesis, DNA/BSA binding, DNA cleavage and cytotoxicity. *BioMetals*, 30:17.  
391 [doi:10.1007/s10534-016-9984-7](https://doi.org/10.1007/s10534-016-9984-7)
- 392 **Zhukova O. S.**, Dobrynin I.V. 2001. Current results and perspectives of the use of human tumor  
393 cell lines for antitumor drug screening. *Voprosy Onkologii*, 47: 706. PMID:11826493

394

395 Supporting Informations

396

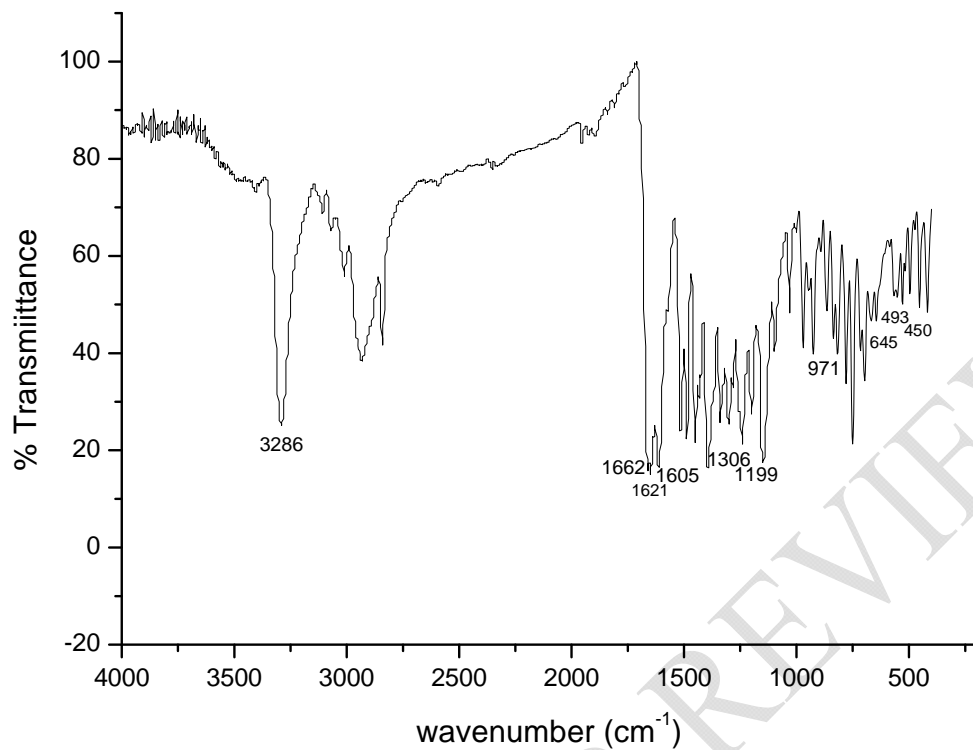


Fig. S1. IR spectrum of the ligand

397

398

399

400

401

402

403

404

405

406

407

408

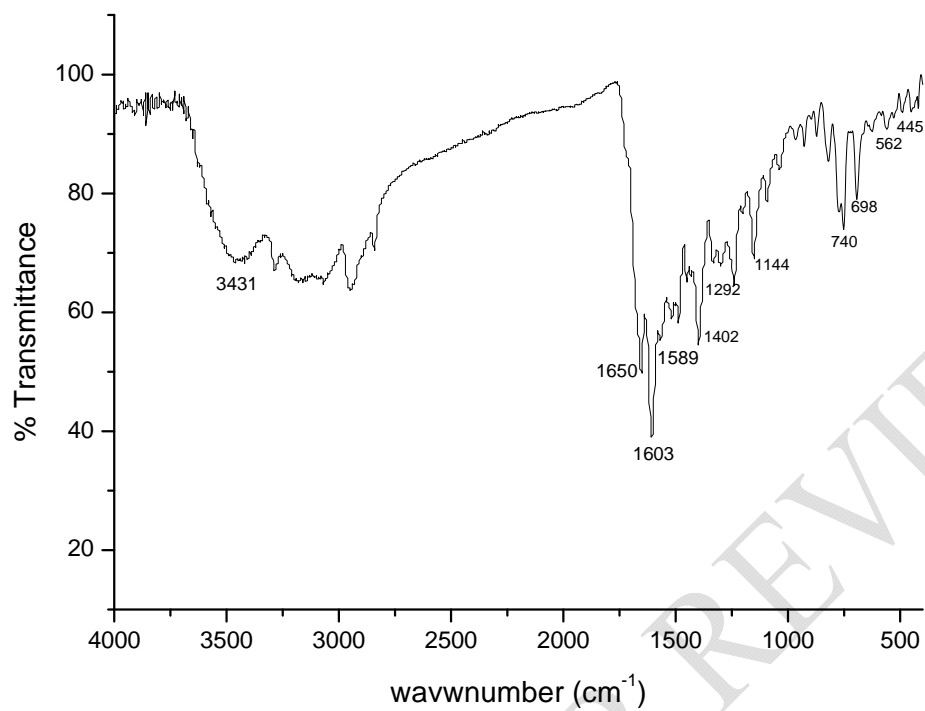
409

410

411



412



413

414

415 Fig. S2. IR spectrum of Pt(II) complex

416

417

418

419

420

421

422

423

424

425

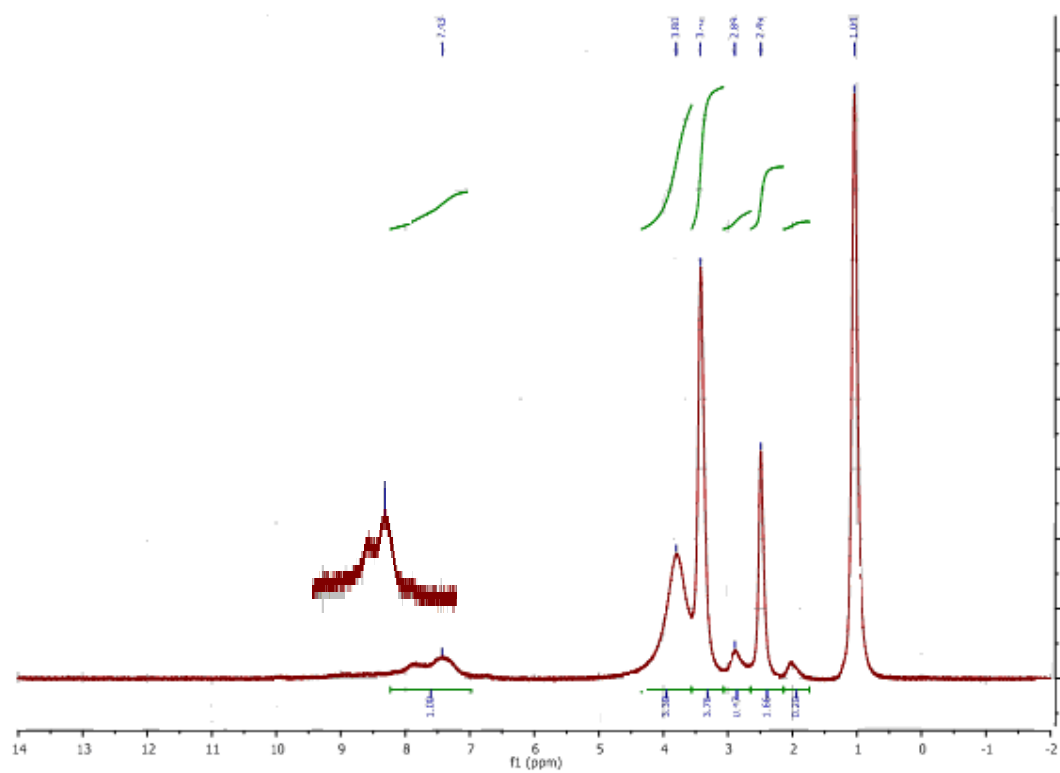
426

427

428

429

430



431

432 Fig. S3. <sup>1</sup>H NMR spectrum of Pt(II) complexes

433

434

435

436

437

438